Applied Catalysis B: Environmental 100 (2010) 346–354

Contents lists available at ScienceDirect

Applied Catalysis B: Environmental

journal homepage: www.elsevier.com/locate/apcatb

Photocatalytic degradation of phenolic compounds with new TiO_2 catalysts

J. Araña [a,*], J.M. Doña-Rodríguez [a,*], D. Portillo-Carrizo [b], C. Fernández-Rodríguez [a], J. Pérez-Peña [a], O. González Díaz [a], J.A. Navío [c], M. Macías [c]

[a] Grupo de Fotocatálisis y Espectroscopía Aplicada al Medioambiente-FEAM (Unidad Asociada al Instituto de Ciencia de Materiales de Sevilla, C.S.I.C.), CIDIA-Depto. de Química, Edificio del Parque Científico Tecnológico, Universidad De Las Palmas De Gran Canaria, Campus Universitario de Tafira, 35017, Las Palmas, Spain
[b] Departamento de Química, Universidad De Zulia, Maracaibo, Venezuela
[c] Instituto de Ciencia de Materiales de Sevilla, Centro Mixto CSIC-Universidad de Sevilla and Departamento de Química Inorgánica, Universidad de Sevilla, Spain

ARTICLE INFO

Article history:
Received 11 June 2010
Received in revised form 30 July 2010
Accepted 5 August 2010
Available online 13 August 2010

Keywords:
TiO_2
Photocatalysis
FTIR
Structure
H_2O_2
Phenolic compounds

ABSTRACT

New TiO_2 catalysts have been synthesised by means of a sol–gel method in which aggregates have been selected before thermal treatment. Sieving and calcination temperature have been proved to be key factors in obtaining catalysts with greater photoactivity than that of Degussa P-25. These new catalysts have been characterized by means of transmission electron microscopy (TEM), BET surface area, diffuse reflectance spectroscopy (DRS), UV–vis spectroscopy, Fourier transformed infrared (FTIR) and X-ray diffraction (XRD). The different parameters studied were compared to those obtained from two commercial catalysts (Degussa P-25 and Hombikat-UV100).

The photocatalytic efficiency of the new catalysts was evaluated by the degradation of various phenolic compounds using UV light (maximum around 365 nm, 9 mW). The catalyst sieved and calcinated at 1023 K, ECT-1023t, showed phenol degradation rates 2.7 times higher than those of Degussa P-25. Also in the degradation of different phenolic compounds, this catalyst showed a higher activity than that of the commercial one. The high photoactivity of this new catalyst has been attributed to the different distribution of surface defects (determined from FTIR studies) and its increased capacity to yield H_2O_2.

1. Introduction

TiO_2 has been the most widely used semiconductor for photocatalytic applications. Several studies have shown that achieving high photocatalytic efficiency with this catalyst requires the consideration of many parameters such as crystal phases, particle size, surface area, particle morphology, distribution of hydroxyl groups, etc. [1–7]. Many researchers consider that the presence of anatase phase is a necessary condition for the process to be effective. However, results from different studies have highlighted the need to combine many aspects, especially when comparing results with the commercial catalyst Degussa P-25. This is considered to be the most efficient photocatalyst for most degradation processes. Its high photoactivity has been mainly attributed to synergistic effects between anatase and rutile phases [8–9]. Nevertheless, catalysts with only anatase phase have shown greater efficiency than Degussa P-25 [10]. Thus, it can be concluded that the appropriate anatase–rutile ratio cannot be considered to be the limiting factor of the process.

Therefore, in order to identify structural parameters that help to improve available photocatalysts, particularly Degussa P-25, many different preparation methods such as flame, sol–gel, hydrothermal or dip-coating synthesis have been developed [10–14]. However, few studies have been able to correlate photoefficiency with structural parameters such as particle size, surface area, particle morphology, faces exposed, acid centres, defects and distribution of hydroxyl groups.

In most studies phenol has been used as a molecule probe for photocatalytic tests due to the fact that its degradation mechanism is well established [1,15–18]. Several authors have been able to correlate the photocatalytic degradation of phenol with the phase composition of the catalysts tested, indicating that the photocatalytic efficiency increases gradually with the content of anatase and its crystallinity [1,19]. Other authors have shown that an increase in the catalyst particle size improves the degradation of phenol [10].

Nonetheless, although many researchers have been able to correlate photocatalytic efficiency with particle size or anatase–rutile ratio, there are many other parameters that affect photocatalytic processes. Thus, determining the role of each physicochemical variable is still a complex task. In this sense, it is difficult to find a material with all the optimum photocatalytic features, particularly because the effect of some can interfere with that of others. For example, catalysts must have a high surface area as this means a

* Corresponding authors. Tel.: +34 928457299; fax: +34 928457397.
E-mail addresses: jaranaesp@hotmail.com (J. Araña), jdona@dqui.ulpgc.es (J.M. Doña-Rodríguez).

0926-3373/$ – see front matter © 2010 Elsevier B.V. All rights reserved.
doi:10.1016/j.apcatb.2010.08.011

greater number of adsorption centres. To achieve high surface area the catalyst's particles must be sufficiently small but this leads to decreased migration time of electrons from the hole to the surface [20,21]. Moreover, a smaller particle size also means a lower crystallinity and therefore a greater number of defects that facilitates the recombination of the e^-/h^+ pair. In addition to this, smaller particles have larger band-gaps and this worsens the photocatalytic efficiency [15,22–25]. Another aspect that must be taken into account is the sort of crystalline planes exposed. Thus, it has been indicated that some planes are more oxidative than others [26].

In this work, new catalysts have been synthesized by means of a sol–gel method by using precursors and reagents which have already been used in other synthesis studies [27,28]. However, in this work, the effect of separating the aggregates after aging and prior to calcination has been evaluated. In this sense, the goal was to determine if this selection could affect the features of the catalyst. As indicated above, phenol is the probe molecule commonly used to test photocatalysts, though activity differences with respect to P25 also depend on the test compound [16]. Thus, photoactivity has been tested and compared to that of Degussa P-25 and Hombikat UV-100 by degradation of several phenolic compounds. The ultimate goal of this study was to determine whether any of the new catalysts brings together the largest number of positive properties to overcome the efficiency of Degussa P-25.

2. Experimental

2.1. Preparation of the catalysts

The new catalysts were synthesized following a sol–gel procedure. For this, an ethanol–titanium butoxide (Panreac (99.5%) and Aldrich (97%) respectively) 50:3.5 ratio molar solution was added drop by drop to a water–ethanol–citric acid (Panreac (99.5%)) 50:60.8:0.36 molar ratio solution. The mixing time was 3 h. After this, the final solution was stirred for 30 min and then allowed to age for 48 h. Then, the catalysts were dried at 373 K, 24 h. After this aging and drying treatment, the effect of separating the aggregates by means of sieving the catalysts with a 63 μm mesh was tested. Larger aggregates than 63 μm were separated from the smaller ones by sieving, resulting in a weight ratio of 53–47%, respectively. The larger aggregates were removed and the smaller ones were calcinated, being these catalysts denominated as sieved. Finally, thin films of the catalysts (282 mg) were placed on porcelain capsules to achieve the complete contact of the catalyst with air during calcination. A 302 K/h slope temperature program was used and the final temperature was held for 3 h. Different synthesis temperatures between 673 and 1073 K were tested.

The new catalysts have been denominated "ECT" (ethanol, citric, tetrabutoxide) followed by the calcination temperature, and to those that have been sieved a "t" has been added at the end of their name.

2.2. Equipment and techniques

For FTIR experiments a spectrophotometer model RS/1 (UNICAM) was used. Intervals of 4000–1000 cm^{-1}, a resolution of 2 cm^{-1} and forward–reverse moving mirrors speed of 10 and 6.2 kHz, respectively were used. These analyses were performed by placing films of the catalysts between two windows of CaF_2. In water interaction studies the catalysts remained in contact with water at the selected pH during 24 h. After this, the catalyst was filtered and water was evaporated at room temperature.

A Philips CM 200 electronic microscope was employed for transmission electron microscopy (TEM) analyses. The microscope was equipped with a top-entry holder and ion pumping system operating at an accelerating voltage of 200 kV and providing a nominal structural resolution of 0.21 nm. Samples were prepared by dipping a 3 mm holed carbon grid into the catalyst suspended in ethanol. Finally, the grids were dried at 323 K for 5 min.

BET surface area measurements were carried out by N_2 adsorption at 77 K using a Micromeritics Gemini instrument.

UV–vis spectra were measured with a Cary 5 (Varian) equipped with an integrating sphere, and using polytetrafluoroethylene (PTFE) as reference. PTFE is considered to be an important material for reflectance studies because of its physic-chemical stability and its high reflectance under any incidence angle. The spectra were recorded in diffuse reflectance mode and transformed to a magnitude proportional to the extinction coefficient (K) by means of the Kubelka–Munk function ($F(R_\infty)$).

X-ray diffraction (XRD) patterns were obtained by using a Siemens D-500 difractometer (Cu K_α, λ = 1.5432 Å). Crystallite sizes in the different phases were estimated from the line broadening of the corresponding X-ray diffraction peaks by using the Scherrer equation. Peaks were fitted by using a Voigt function.

A 60 W Philips Solarium HB175 equipped with four 15 W Philips CLEO fluorescent tubes with emission spectrum from 300 to 400 nm (maximum around 365 nm) (9 mW) was used as UV source in degradation studies of phenolic compounds. The remaining concentrations of the compounds at different reaction times were HPLC-measured using a Supelco Discovery C18 25 cm × 4.6 mm ID, 5 μm particles column and an acetonitrile–water (20:80) as mobile phase, using a UV detector (λ = 270 nm) for analysis of phenol and intermediates. The concentration of H_2O_2 was monitored by HPLC at λ a 210 nm.

2.3. Reaction conditions

Aqueous suspensions containing 0.53 mM of phenolic compound and 1 g/l catalysts in 250 ml glass vessels were continuously stirred and air-bubbled (400 ml/min). All the experiments were performed at constant pH 5 and room temperature. The organics chemisorption on the catalyst surface was favoured by air-bubbling and stirring for 30 min before switching on the UV-lamp. Degradation rates were calculated by using the Langmuir–Hinshelwood model which provided high regression coefficients (0.989–0.999). The reproducibility of results in terms of error was less than 1%.

3. Results and discussion

3.1. Characterization studies

3.1.1. Structural and surface area characterization studies

Different studies have shown that calcination temperature is crucial in catalyst synthesis as it controls, among other processes, the transformation of anatase to rutile. It is known that anatase is more stable at temperatures among 573–823 K, while rutile phase is more stable at higher temperatures [1]. It has also been indicated that anatase–rutile thermal transition depends on the presence of foreign elements [29]. However, in addition to temperature there are other parameters that determine catalysts' structural features and phase conversion such as particle size and surface defects or the route of preparation [30]. In fact, some studies have suggested that the thermodynamic stability of TiO_2 phases depends, among other variables, on the particle diameter being anatase the most stable phase for particle sizes below 14 nm and rutile above 35 nm [31,32]. Other authors have indicated that the presence of defects determines the particle size at which the transformation of anatase to rutile occurs. In addition to this, the critical particle size for which anatase transforms to rutile varies with calcination temperature [33]. Thus, most studies reveal that particle size is

Table 1
Band-gap, surface area, crystalline size and percentage of anatase-rutile phases in the different catalysts.

Catalyst	Anatase (A)/rutile (R) ratio	Crystalline size (nm) (A)	Crystalline size (nm) (R)	Surface area (m^2/g)	Band-gap (eV)
Degussa P-25	80% A/20% R	22	25	52	3.18
Hombikat-UV100	100% A	7	–	280	3.22
ECT-673t	100% A	11.9	–	62.99	3.20
ECT-673	100% A	13.2	–	63.0	3.20
ECT-773t	100% A	21.7	–	38.4	3.19
ECT-773	100% A	21.7	–	38.3	3.19
ECT-873	100% A	38.8	–	27.7	3.19
ECT-873t	100% A	36.9	–	27.8	3.19
ECT-973	96–97% A/4–3% R	49.1	62.2	19.3	3.17
ECT-973t	96–98% A/4–2% R	50.0	101.6	19.2	3.17
ECT-1023	87–93% A/13–7% R	57.0	87.1	18.3	2.97
ECT-1023t	89–94% A/11–6% R	57.0	86.3	18.3	2.97
ECT-1073	34–27% A/73–66% R	76	104	9.7	2.96
ECT-1073t	20–30% A/80–70% R	62.3	96.1	9.7	2.96

a key parameter in controlling this thermodynamic transformation.

Table 1 shows the distribution of anatase and rutile phases, particle size and surface areas of the new catalysts and compared to those of the commercial Degussa P-25 or Hombikat UV-100. First of all, it should be noted that regarding these parameters the effect of sieving was negligible. Secondly, it is noteworthy that surprisingly, the catalysts calcinated at 973 and 1023 K contained low rutile, even when anatase particle size was 50 and 57 nm for ECT-1023 and ECT-1023t. Moreover, as can be expected at higher calcination temperatures there were a progressive decrease in surface area with increasing particle size. Accordingly, ECT-1023's surface is almost 3.5 times lower than that of ECT-673.

Additionally, none of the synthesized catalysts have the same anatase–rutile ratio, particle size and surface area than those of the commercial catalysts.

3.1.2. Diffuse reflectance UV–vis spectra characterization

In this study, diffuse reflectance spectra of new catalysts have been carried out and band-gap values have been determined from them (Table 1). As can be observed, at higher calcination temperatures the obtained band-gaps of the new catalysts become slightly decreased. This effect has also been observed in other studies, in which increased band-gaps were correlated with decreased particle size and crystallinity, resulting in faster e^-/h^+ recombination [15,34].

3.1.3. TEM characterization studies

TEM has been used in numerous catalyst morphology characterization studies. The literature has placed great emphasis on highlighting the photocatalytic efficiency of anatase compared to that of rutile. However, not all particles having anatase phase have similar properties. During the synthesis of the catalysts, the growth of a certain phase can be prompted. This would lead to different anatase crystallographic faces with dissimilar surface active centre distribution [35,36]. Thus, for the proper characterization of the new catalysts, TEM studies were performed. Fig. 1 compares the image of the sieved catalysts with those of the commercial catalysts.

These results confirm the gradual increase of particle size with increasing calcination temperature. In addition to this, the improvement of polyhedral morphology with increasing temperature becomes apparent, so that the particles of catalysts calcinated at temperatures greater or equal to 973 K show truncated square bipyramidal morphology with almost perfect square base. However, particles of Degussa P-25, Hombikat UV-100 and catalysts calcinated at lower temperatures are almost spherical.

Different thermodynamic studies have determined that the most favourable crystalline form of anatase phase is a truncated bipyramid with a square base in which the exposed surface faces are mainly (1 0 1) and (0 0 1) [36–38]. This is the case for ECT-973t, ECT-1023t and ECT-1073t. In fact, thermodynamic equilibriums have revealed that the more stable faces of anatase structure are (1 0 1) and (0 0 1) whatever the pressure and temperature of synthesis [36]. However, certain pressures and temperatures do not allow the presence of faces (1 1 0) or (1 0 0) [36]. Additionally, slight modifications of these variables change the proportion of faces (1 0 1) and (0 0 1). This indicates that at low water pressures, increased temperature favours the growth of face (1 0 1) because the elimination of OH groups of the face (0 0 1) results in an increased surface energy and consequently a decreased area. In this regard, most particles observed in catalysts calcinated at $T \geq 973$ K show the more or less homogeneous growth of all exposed faces. The synthesis method used including the calcination process in which the surface of the catalysts was well exposed to air seems to have favoured the morphology observed.

3.1.4. Characterization of surface hydroxyl groups

Various studies have shown that the analysis of the surface distribution of hydroxyl groups can highlight the faces predominantly exposed to the catalyst's surface [37]. Different faces show different distribution of such groups and therefore different active sites. The knowledge of surface hydroxyl group distribution is important because water molecules are always present on these catalysts' surfaces and additionally because their distribution can help to understand their photocatalytic behaviour. Different models have been proposed for anatase surface. Some authors [38,39] found that face (0 0 1) is the one predominantly exposed indicating that the band of the hydroxyl groups at higher wavenumber is attributed to isolated hydroxyl groups present on such faces [37]. These isolated hydroxyl groups are characteristic of defects or oxygen vacancies on the catalyst surface. Moreover, the hydroxyl groups appearing at lower wavenumbers (3660 or 3675 cm^{-1}) are thought to be attached to neighbouring titanium atoms [40]. It has also been indicated that in Degussa P-25, face (0 0 1) is the one more frequently exposed. Thus, in order to compare the surface distribution of hydroxyl groups, spectra between 4000 and 1000 cm^{-1} have been performed for these catalysts (Fig. 2).

In samples Degussa P-25, ECT-673t, ECT-773t and ECT-873t, the band at 3698 cm^{-1} attributed to isolated hydroxyl groups present on the face (0 0 1) and surface defects can be clearly distinguished [36,37]. A broad band between 3690 and 3000 cm^{-1} was observed and attributed to hydroxyl groups located close to each other. Such a broad band can also be attributed to water molecules adsorbed by means of hydrogen bond or by Ti^{4+} atoms, most probably to the face (1 0 1) [37,41,42]. In the sieved catalysts calcinated at 973 K and higher temperatures, the band at 3698 cm^{-1} was not observed. It

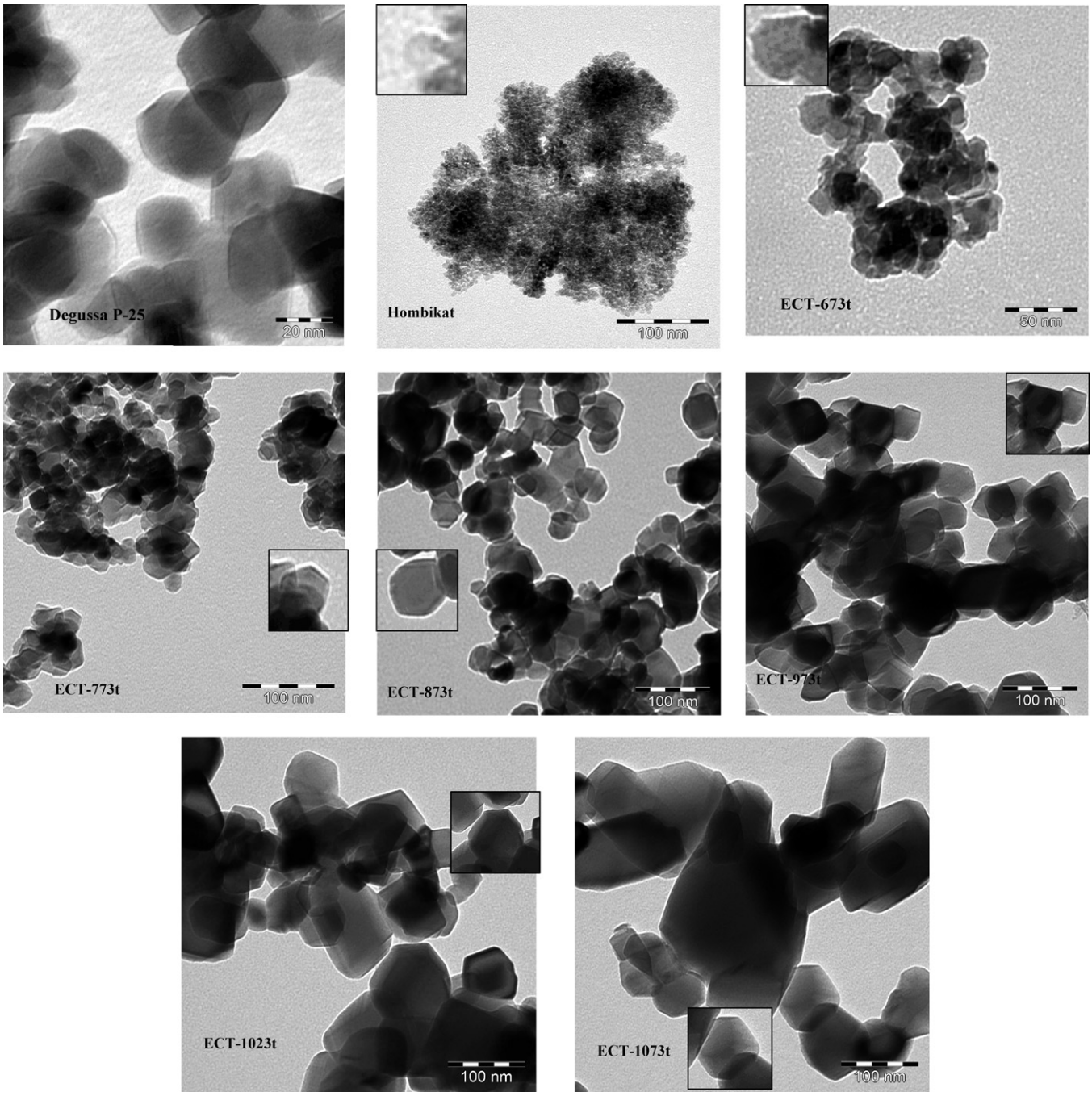

Fig. 1. TEM photograms. In some photograms a particle has been selected and amplified.

has been indicated that increasing anatase particle size decreases the number of surface defects leading to lower recombination rate of the e^-/h^+ couple [15]. In the catalysts sieved there is a correspondence between the presence of isolated hydroxyl groups and the particle size that could be correlated with the number of surface defects. However, the catalysts calcinated at $T \geq 973$ K but not sieved seem to have more surface defects, as their spectra show the bands of isolated hydroxyl groups, even when they present the same characteristics of those sieved in terms of particle size and surface area. Hombikat does not contain isolated hydroxyl groups and bands in the region between 3690 and 2600 cm^{-1} show different relative intensities from those of the other catalysts.

To achieve a better characterization of these sites, FTIR studies of the interaction of water with the surface of different catalysts at different pH were carried out. Degussa P-25 and ECT-873t were selected because of the presence of isolated hydroxyl groups and ECT-1023t because of their absence (Fig. 3(1) and (2)).

Spectra from Degussa P-25 (Fig. 3(1)) show an increase of the band at 3698 cm^{-1} and those attributed to the presence of water among 3690, 3000 and 1640 cm^{-1}. At pH > 7, the intensity of the band centred at 3100 cm^{-1} was increased and further greater increments in intensity of the band at 1640 cm^{-1} lead to the formation of shoulder around 1630 cm^{-1}.

No changes with respect to the original spectrum were observed from the interaction of water with ECT-873t at any pH. However, when ECT-1023t adsorbed water at pH lower than 7 (Fig. 3(2)), isolated hydroxyl groups (band at 3698 cm^{-1}) were generated in addition to new bands between 3400 and 3200 cm^{-1}. However,

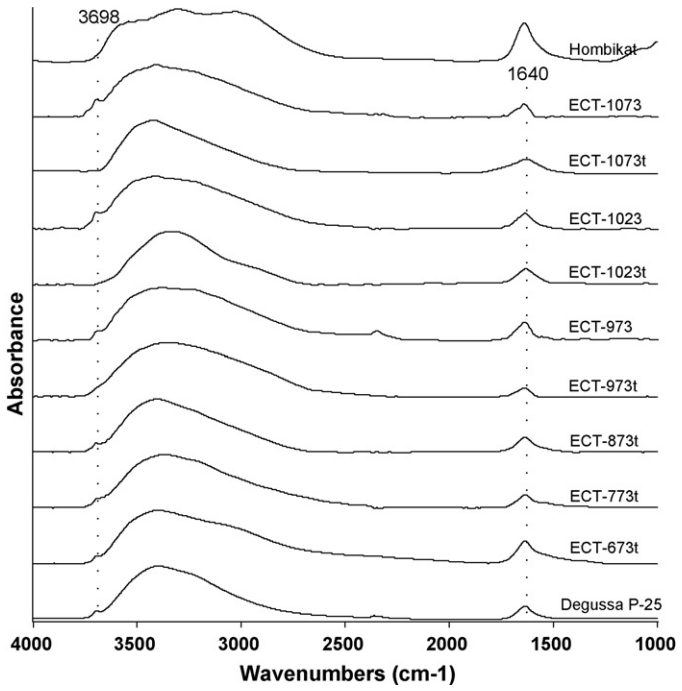

Fig. 2. FTIR spectra from the distribution of hydroxyl groups and water adsorbed.

the intensity of the water band at 1640 cm^{-1} was not incremented suggesting that water adsorption was negligible. At pH > 7 the band attributed to isolated hydroxyl groups was not visible but a shift of the broad band towards lower wavenumbers 3250 cm^{-1} was observed. Other studies have indicated that the adsorption of water on the surface of anatase's face (0 0 1) is dissociative leading to the breakdown of Ti–O–Ti bonds [35,43] and the formation of Ti–OH bonds, i.e., typical isolated hydroxyl groups. This formation mechanism of isolated hydroxyl groups from the interaction of water occurs mainly in ECT-1023t at pH ≤ 7 and in Degussa P-25. To determine the stability of these centres, ECT-1023t and Degussa P-25 were dried at 373 K and then again analyzed by FTIR spectroscopy. For ECT-1023t, the resulting spectra did not contain isolated hydroxyl groups, i.e., they were similar to those obtained before the interaction with water. This indicates that drying the catalysts regenerates their initial surface.

3.2. Degradation studies

3.2.1. Phenol photocatalytic degradation

Fig. 4 shows the apparent rate constants for the degradation of phenol (k_{Ph}) with the different catalysts. As can be observed, the values of k_{Ph} for the new catalysts (sieved and not sieved) increased progressively with increasing calcination temperature, up to 1023 K. However, at higher temperatures rate constants decrease dramatically.

It is noteworthy that k_{Ph} for Degussa P-25 is 2.7 times lower than that for ECT-1023t. Moreover, surface area of ECT-1023t is much smaller than that of the commercial catalyst. If surface area is considered, the resulting k_{Ph} for this catalyst is more than 7 times greater than that for Degussa P-25.

As shown in Fig. 4, the higher the anatase particle size the greater the values of k_{Ph}. Only ECT-1073t does not follow this trend. This is probably due to its low anatase phase ratio (<35%), as obtained from the characterization study. These results agree with those obtained by Agrios and Pichat [16] who also observed a significant degradation rate increment for phenol as particle size were increased, but not as marked as that obtained in this study. These authors worked with commercial catalysts (Millennium Chemical titania) PC10. PC50, PC105 and PC500, with surface areas of 10, 54, 85–90 and 317 m^2/g, respectively and particle sizes of 65–75, 20–30, 15–25 and 5–10 nm, respectively. Such study attributed the improved photocatalytic efficiency to the lower number of defects provided by the higher crystallinity at higher calcination temperatures. Fewer defects mean lower e^-/h^+ recombination rate and higher production of radicals. The defect states can be understood from the following relations [44]:

$$TiO_2 \rightarrow TiO_2(e^-/h^+)(e^-_{CB} + h^+_{VB}) \quad (1)$$

$$V_0^O + e_{CB}{}^- \rightarrow V_0(e^-) \quad (2)$$

$$V_0 + h_{VB}{}^+ \rightarrow V_0^O + h\nu \quad (3)$$

Furthermore, our new catalysts also showed a significant decrease in the concentration of isolated surface hydroxyl groups with increasing calcination temperature. These groups are located at defects and/or oxygen vacancies on the surface [45]. That is, cata-

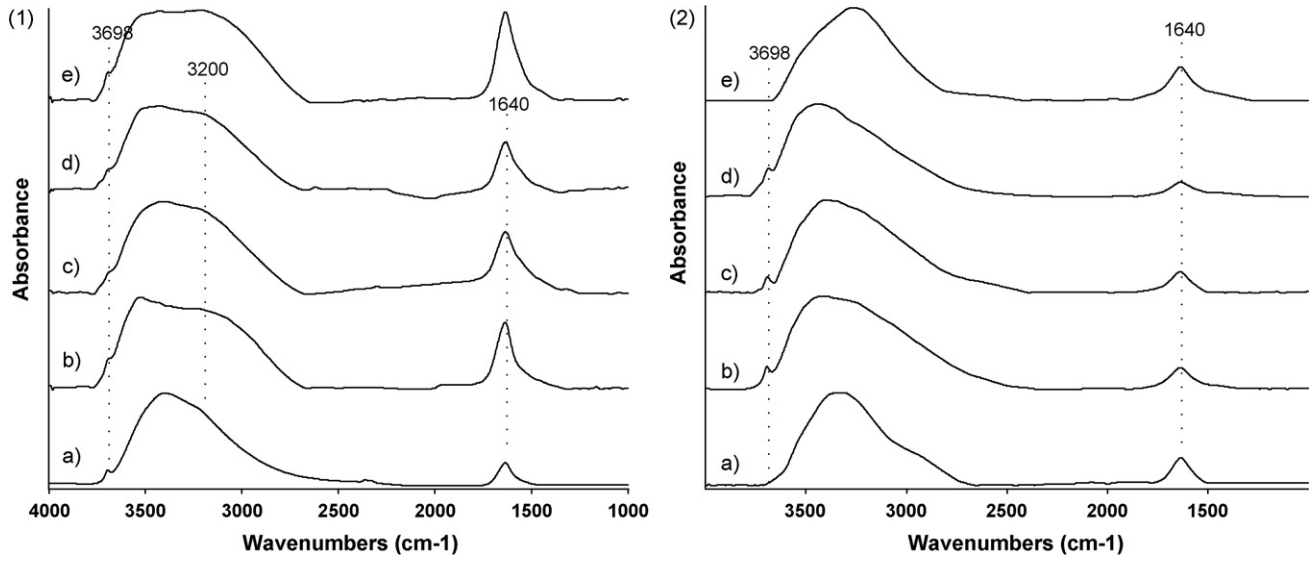

Fig. 3. FTIR spectra from the interaction of water at different pH with Degussa P-25 (1) and ECT-1023t (2). (a) reference spectrum, (b) pH 3, (c) pH 5, (d) pH 7 and (e) pH 9.

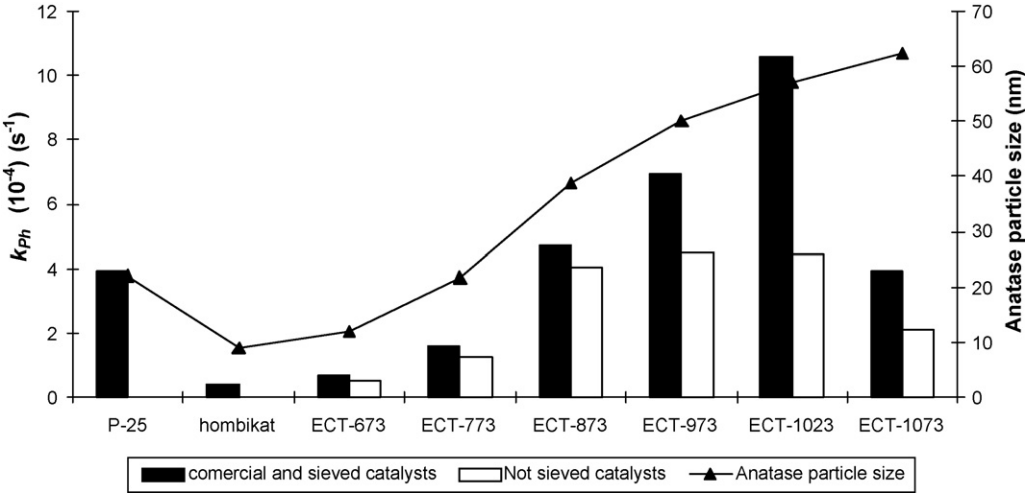

Fig. 4. Apparent first-order rate constants from phenol degradation compared to anatase particle size.

lysts calcinated at higher temperature have fewer defects and e^-/h^+ recombination rate will also be lower which should favour the formation of radicals. The characterization studies have also shown the formation of isolated hydroxyl groups as a result of the interaction and breaking of the water molecule in certain centres. This process may be responsible for radical formation, as well.

The values of k_{Ph} for sieved catalysts calcinated at temperatures lower than 873 K (Fig. 1) are slightly higher than those for catalysts not-sieved and calcinated at the same temperatures. Yet, at higher calcination temperatures, k_{Ph} for sieved catalysts almost doubles those for not-sieved ones. FTIR characterization studies for catalysts not-sieved and calcinated at temperatures above 873 K showed that the distribution of isolated hydroxyl groups was similar to the one observed for sieved catalysts at temperatures below 873 K. As mentioned above, these groups are present in defects or oxygen vacancies of the catalyst surface. This would indicate that not-sieved catalysts host an increased number of defects that leads to higher recombination rate and less degradation. In conclusion, sieving the catalyst is capital for improving its photoefficiency, as this process helps to remove the larger aggregates formed before calcination. This shows that the selection of aggregate size before calcination does not change parameters such as particle size, band-gap or surface area but the number of surface defects determined from the presence of isolated hydroxyl groups. The smaller size of the aggregates seems to improve the access of air to the whole surface of the catalyst during the thermal treatment leading to the generation of fewer defects.

3.2.2. Phenol photocatalytic mineralization

Mineralization is another important process to be considered in wastewater treatment as it assures the elimination of the pollutant and its intermediates. In fact, the intermediates of the photocatalytic degradation of phenol (hydroquinone and catechol) are more toxic than phenol. Fig. 5 shows the evolution of the apparent mineralization kinetic constant (k_{TOC}) for phenol degradation.

As can be observed, the evolution of k_{TOC} is similar to that of k_{Ph} with higher values at increasing calcination temperatures up to 1023 K. Only k_{TOC} for ECT-1023t is greater than that for Degussa P-25. Furthermore, the catalysts calcinated at higher temperatures and sieved provided greater mineralizations. In another study in which commercial catalysts with different surface areas and particle size were compared, no correlation was observed between degradation and particle size or degradation and mineralization [46]. Such study indicated that catalysts with lower surface area provided lower mineralization rates. As shown in Fig. 5, correlation between k_{Ph} and k_{TOC} is not perfect. However, the picture is rather different when the same constants are calculated by considering surface area with the sieved catalysts. Moreover, this figure shows that for catalysts with smaller particle size (<25 nm) the values of k_{Ph} and k_{TOC} were very similar. Nonetheless, as particle size increased, differences between both constants became also gradually augmented. Most intermediates of phenol degradation are degraded by hydroxyl radical attack but some of them, such as carboxylic acids can be degraded by the Kolbe reaction [47]. Catalysts calcinated at higher temperatures showed the greatest differences between k_{Ph} and k_{TOC}.

3.2.3. Phenol photocatalytic intermediates

The evolution of catechol and hydroquinone during the photocatalytic treatment of phenol was also monitored. Fig. 6(1) and (2) shows the obtained results during the first 90 min of reaction with Degussa P-25 and that catalyst which showed a higher activity (ECT-1023t).

The formation of catechol during the first 30 min with ECT-1023t was higher than with Degussa P-25. However, at longer reaction times the evolutions of the concentration of this intermediate with both catalysts were similar. The higher concentration of catechol dissolved in the studies with ECT-1023t could be due to the catalyst's smaller surface and lower hydroxylation. Since catechol forms chelates with surface OH groups [48], its uptake by the catalyst's surface will be lower. During the first 30 min of reaction, the concentration of hydroquinone was also higher in the ECT-1023t, but at longer reaction times it became greater for the commercial catalyst.

The effect of the presence of H_2O_2 on the degradation of phenol with ECT-1023t and Degussa P-25 was also studied. With the former, the process was slightly improved, as k_{Ph} varied from 3.93×10^{-4} to $4.81 \times 10^{-4}\ s^{-1}$ after the addition of the peroxide. However, in the case of ECT-1023t the presence of H_2O_2 slowed down phenol degradation with k_{Ph} being reduced from 10.6×10^{-4} to $9.34 \times 10^{-4}\ s^{-1}$). It is worthwhile noting that the evolution of catechol and hydroquinone (Fig. 6(1) and (2)) in the presence of H_2O_2 with both catalysts was the same as that observed in the ECT-1023t without this oxidant.

During a photocatalytic process, H_2O_2 can be produced from the reduction of O_2 by two electrons. Hydrogen peroxide may react with the photogenerated electrons to produce hydroxyl radicals (4) or react with them to yield hydroperoxide radicals (5):

$$H_2O_2 + e^- \rightarrow {}^{\bullet}OH + OH^- \quad (4)$$

$$H_2O_2 + {}^{\bullet}OH \rightarrow HO_2^{\bullet} + H_2O \quad (5)$$

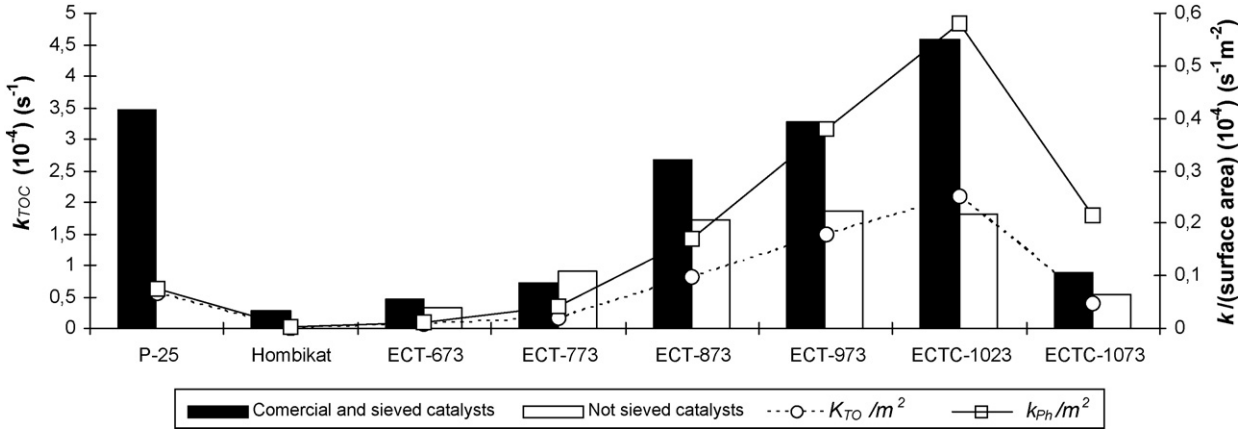

Fig. 5. Apparent first-order rate constants from phenol mineralization compared to k_{Ph}/surface area and k_{TOC}/surface area.

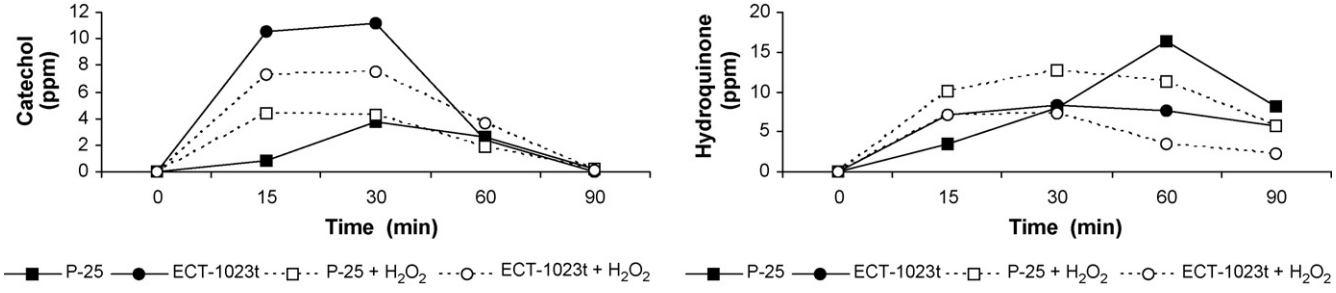

Fig. 6. Catechol (1) and hydroquinone (2) concentration during phenol degradation studies with Degussa P-25 and ECT-1023t.

Some authors have indicated that there is an optimal concentration of H_2O_2 that provides the surface coating to achieve the best photocatalytic efficiency [49]. Owing to the fact that the distributions of the phenol degradation intermediates (catechol and hydroquinone) in the studies with H_2O_2 were similar to those with ECT-1023t without the peroxide, the concentration of H_2O_2 was monitored during the degradation of phenol (Fig. 7).

As can be observed, the concentrations of the peroxide obtained with ECT-1023t were notably greater than those with Degussa P-25. The higher production of H_2O_2 by ECT-1023t and the catalysts sieved and calcinated at higher temperatures can help to explain the significant difference between k_{Ph} and k_{TOC} shown in Fig. 5. In fact, the presence of H_2O_2 hindered the mineralization of phenol.

3.2.4. Degradation of phenolic compounds

As shown above, the catalyst ECT-1023t provides faster degradation of phenol and greater formation of H_2O_2 than those of Degussa P-25. To improve our understanding of the behaviour of the new catalyst, the degradation of other phenolic compounds with this catalyst was studied and compared to that with Degussa P-25.

Fig. 8 illustrates surface degradation constant rates (degradation constant rates divided by the catalyst's surface, $k_{Ph/surf}$) for phenol, catechol resorcinol, hydroquinone, *o*-aminephenol, *m*-aminephenol, *p*-aminephenol, *o*-cresol, *m*-cresol and *p*-cresol with Degussa P-25 and ECT-1023t.

In all cases, the obtained values of $k_{Ph/surf}$ for ECT-1023t are greater than those for Degussa P-25. With ECT-1023t, the observed

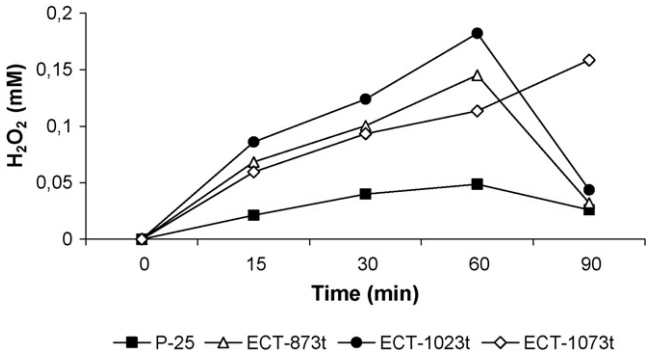

Fig. 7. Concentration of H_2O_2 produced during degradation phenol.

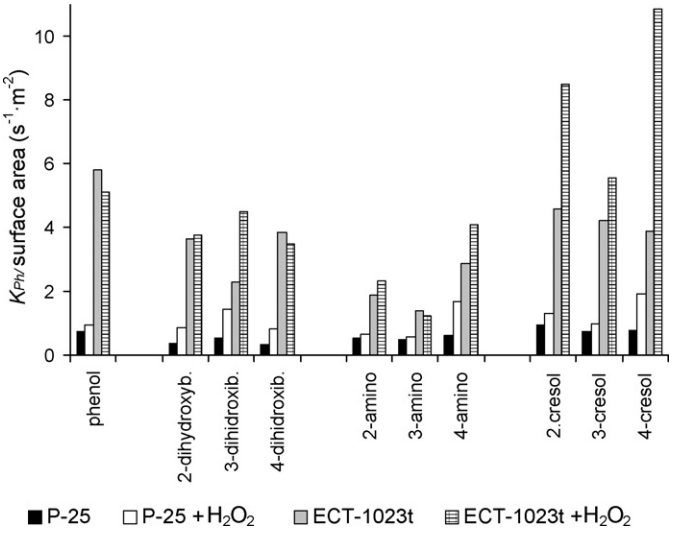

Fig. 8. Apparent first-order rate constants/surface area from different phenolic compounds degradation.

degradation rates for the different groups of compounds follow the sequence: cresols > dihydroxybenzenes > aminophenols. Nonetheless, with P-25 the degradation of aminophenols was faster than those of dihydroxybenzenes. For these phenolic compounds, degradation rates did not seem to follow a perfect correlation with the Hammett constants. As mentioned in the introduction, there are many other factors that can influence the process. Additionally, other studies have indicated that depending on the molecule under study, the crystallinity of the catalyst can vary the sequence of degradation rates [16].

These experiments were also carried out in the presence of H_2O_2. In the degradation of aminophenols with ECT-1023t with and without H_2O_2, the *meta* position was not favoured with respect to *ortho* and *para* positions. However, with P-25, the *meta* position was not favoured only in the presence of the peroxide. This means that the behaviour of P-25 with H_2O_2 is similar to that of ECT-1023t without H_2O_2.

In the case of the dihydroxybenzenes with ECT-10233t, the presence of H_2O_2 hampered degradation for positions *orto* and *para*, which is the opposite of that observed with P-25. This effect could be explained by interferences probably generated by reaction (5). Nevertheless, for cresols the effect of H_2O_2 was more significant for ECT-1023t than for the commercial catalyst. These results indicate that the H_2O_2 formed during the photocatalytic process plays a significant role in the degradation of the studied compounds, being more effective in the case of the new catalyst.

Moreover, as stated above, photocatalytic reactions also depend on the catalyst's exposed face, oxidation process being promoted on face 0 0 1 and reduction process on face 1 0 1 [50]. The characterization and degradation studies performed in this work suggest that the promoted surface faces of the new catalysts are different from those of Degussa P-25, leading to different degradations.

4. Conclusions

This study has shown that the removal of larger aggregates before calcination by means of sieving, a correct aeration and calcination temperature leads to the development of new catalysts with well defined photocatalytic properties. The obtained results suggest that sieving the catalyst does not alter particle size, surface area or phase distribution. However, the effect on surface defects depends on the calcination temperature. The new sieved catalysts are characterised by great anatase content and particle size, but apparently low concentration of surface defects as determined from FTIR analyses of the isolated hydroxyl groups.

The catalyst calcinated at 1023 K and sieved, ECT-1023t, showed a greater efficiency at the degradation of different phenolic pollutants than that of Degussa P-25. This greater efficiency can be attributed to the fact that ECT-1023t:

- generates more isolated hydroxyl groups and oxygen vacancies from the interaction of its surface with water,
- provides more H_2O_2 during the photocatalytic process than P-25,
- has larger particles that lead to lower e^-/h^+ recombination rates and band-gap (2.96 eV),
- contains a low proportion of rutile phase, which can affect charge transfer processes.

The higher photocatalytic efficiency in the degradation of phenolic compounds provided by ECT-1023t, as a result of the features described in this paper is a promising result for the efficient application of photocatalysis.

Acknowledgments

We are grateful for the funding of the European Commission through the Clean Water Project which is a Collaborative Project (Grant Agreement number 227017) co-funded by the Research DG of the European Commission within the joint RTD activities of the Environment and NMP Thematic Priorities. Furthermore, we wish to thank the Spanish Ministry of Science and Innovation for their financial support through the Project CTQ2008-05961-C02-02, CTQ2008-05961-C02-01, to the FONACIT of Venezuela for their financial support to Mr. D. Portillo and microscopy service of ULPGC.

References

[1] Z. Ambrus, K. Mogyorósi, Á. Szalai, T. Alapi, K. Demeter, A. Dombi, P. Sipos, Appl. Catal. A: Gen. 340 (2008) 153–161.
[2] A. Fujishima, X. Zhang, D.A. Tryk, Surf. Sci. Rep. 63 (2008) 515–582.
[3] Y. Bessekhouad, D. Robert, J.V. Weber, J. Photochem. Photobiol. A: Chem. 157 (2003) 47–53.
[4] L. Gao, Q. Zhang, Scripta Mater. 44 (2001) 1195–1198.
[5] S. Tsai, S. Cheng, Catal. Today 33 (1997) 227–237.
[6] J. Araña, C. Garriga i Cabo, J.M. Doña-Rodríguez, O. González-Díaz, J.A. Herrera-Melián, J. Pérez-Peña, Appl. Surf. Sci. 239 (2004) 60–71.
[7] J. Araña, J.M. Doña Rodríguez, O. González Díaz, J.A. Herrera Melián, C. Fernández Rodríguez, J. Pérez Peña, Appl. Catal. A: Gen. 299 (2006) 274–284.
[8] D.C. Hurum, A.G. Agrios, K.A. Gray, T. Rajh, M.C. Thurnauer, J. Phys. Chem. B 107 (2003) 4545–4549.
[9] G. Colón, J.M. Sánchez-España, M.C. Hidalgo, J.A. Navío, J. Photochem. Photobiol. A: Chem. 179 (2006) 20–27.
[10] N. Balázs, K. Mogyorósi, D.F. Srankó, A. Pallagi, T. Alapi, A. Oszkó, A. Dombi, P. Sipos, Appl. Catal. B: Environ. 84 (2008) 356–362.
[11] C.L. Yeha, S.H. Yehb, H.K. Ma, Powder Technol. 145 (2004) 1–9.
[12] M.C. Hidalgo, M. Aguilar, M. Maicu, J.A. Navío, G. Colón, Catal. Today 129 (2007) 50–58.
[13] A.I. Kontos, A.G. Kontos, D.S. Tsoukleris, G.D. Vlachos, P. Falaras, Thin Solid Films 515 (2007) 7370–7375.
[14] N. Negishi, S. Matsuzawa, K. Takeuchi, P. Pichat, Chem. Mater. 19 (2007) 3808–3814.
[15] S. Liu, N. Jaffrezic, C. Guillard, Appl. Surf. Sci. 255 (2008) 2704–2709.
[16] A.G. Agrios, P. Pichat, J. Photochem. Photobiol. A: Chem. 180 (2006) 130–135.
[17] J. Araña, J.M. Doña-Rodríguez, E. Tello Rendón, C. Garriga i Cabo, O. González-Díaz, J.A. Herrera-Melián, J. Pérez-Peña, G. Colón, J.A. Navío, Appl. Catal. B: Environ. 44 (2003) 153–160.
[18] C. Renzi, C. Guillard, J. Herrmann, P. Pichat, G. Baldi, Chemosphere 35 (1997) 819–826.
[19] B. Tryba, M. Toyoda, A.W. Morawski, R. Nonaka, M. Inagaki, Appl. Catal. B: Environ. 71 (2007) 163–168.
[20] Z. Zhang, C. Wang, R. Zakaria, J.Y. Ying, J. Phys. Chem. B 102 (1998) 10871–10878.
[21] N. Serpone, D. Lawless, R. Khairlutdinov, E. Pelizzetti, J. Phys. Chem. B 99 (1995) 16655–16661.
[22] P. Pichat, R. Enriquez, E. Mietton, Solid State Phenom. 162 (2010) 41–48.
[23] P. Rivera, K. Tanaka, T. Hisanaga, Appl. Catal. B: Environ. 3 (1993) 37–44.
[24] A.J. Maira, K.L. Yeung, C.Y. Lee, P.L. Yue, C.K. Chan, J. Catal. 192 (2000) 185–196.
[25] C. Minero, D. Vione, Appl. Catal. B 67 (2006) 257–269.
[26] F. Amano, T. Yasumoto, O. Prieto-Mahaney, S. Uchida, T. Shibayama, B. Ohtani, Chem. Commun. (2009) 2311–2313.
[27] Y. Hao, Q. Lai, D. Liu, Z. Xu, X. Ji, Mater. Chem. Phys. 94 (2005) 382–387.
[28] V. Vinothini, P. Singh, M. Balasubramanian, Ceram. Int. 32 (2006) 99–103.
[29] A.M. Ruiz, A. Cornet, J.R. Morante, Sens. Actuator B 100 (2004) 256–260.
[30] O. Carp, C.L. Huisman, A. Reller, Prog. Solid State Chem. 32 (2004) 33–177.
[31] P. Billik, G. Plesch, Mater. Lett. 61 (2007) 1183–1186.
[32] H. Zhang, J.F. Banfield, J. Phys. Chem. B 104 (2000) 3481–3487.
[33] L. Gonzalez-Reyes, I. Hernández-Pérez, F.C. Robles Hernández, H. Dorantes Rosales, E.M. Arce-Estrada, J. Eur. Ceram. Soc. 28 (2008) 1585–1594.
[34] P. Calza, E. Pelizzetti, K. Mogyorósi, R. Kun, I. Dékány, Appl. Catal. B: Environ. 72 (2007) 314–321.
[35] S. Dzwigaj, C. Arrouvel, M. Breysse, C. Geantet, S. Inoue, H. Toulhoat, P. Raybaud, J. Catal. 236 (2005) 245–250.
[36] C. Arrouvel, M. Digne, M. Breysse, H. Toulhoat, P. Raybaud, J. Catal. 222 (2004) 152–166.
[37] G. Munuera, F. Moreno, F. Gonzalez, in: J.S. Anderson, M.W. Roberts, F.S. Stone (Eds.), Reactivity of Solids, Chapman Hall, London, 1972.
[38] M. Primet, P. Pichat, M.V. Mathieu, J. Phys. Chem. 75 (1971) 1216–1220.
[39] C. Arrouvel, H. Toulhoat, M. Breysse, P. Raybaud, J. Catal. 226 (2004) 260–272.
[40] G. Martra, Appl. Catal. A: Gen. 200 (2000) 275–285.
[41] G. Busca, H. Saussey, O. Saur, J.-C. Lavalley, V. Lorenzelli, Appl. Catal. 14 (1985) 245–260.
[42] C. Morterra, J. Chem. Soc., Faraday Trans. 1 (84) (1988) 1617–1637.
[43] A. Vittadini, A. Selloni, F.P. Rotzinger, M. Gratzel, Phys. Rev. Lett. 81 (1998) 2954–2957.

[44] P.M. Kumar, Thin Solid Films 358 (2000) 122–130.
[45] A.A. Bonapasta, F. Filippone, G. Mattioli, P. Alippi, Catal. Today 144 (2009) 177–182.
[46] D. Gumy, S.A. Giraldo, J. Rengifo, C. Pulgarin, Appl. Catal. B: Environ. 78 (2008) 19–29.
[47] B. Kraeutler, A.J. Bard, J. Am. Chem. Soc. 99 (1977) 7729–7731.
[48] X. Li, J.W. Cubbage, W.S. Jenks, J. Org. Chem. 64 (1999) 8525–8536.
[49] B. Jenny, P. Pichat, Langmuir 7 (1991) 947–964.
[50] N. Murakami, Y. Kurihara, T. Tsubota, T. Ohno, J. Phys. Chem. C 113 (2009) 3062–3069.